

Automated Layout Design and Control of Robust Cooperative Grasped-Load Aerial Transportation Systems

Carlo Bosio, Jerry Tang, Ting-Hao Wang, and Mark W. Mueller

Abstract— We present a novel approach to cooperative aerial transportation through a team of drones, using optimal control theory and a hierarchical control strategy. We assume the drones are connected to the payload through rigid attachments, essentially transforming the whole system into a larger flying object with “thrust modules” at the attachment locations of the drones. We investigate the optimal arrangement of the thrust modules around the payload, so that the resulting system is robust to disturbances. We choose the \mathcal{H}_2 norm as a measure of robustness, and propose an iterative optimization routine to compute the optimal layout of the vehicles around the object. We experimentally validate our approach using four drones and comparing the disturbance rejection performances achieved by two different layouts (the optimal one and a sub-optimal one), and observe that the results match our predictions.

I. INTRODUCTION

The increasing demand for effective and autonomous transportation in applications such as logistics, search and rescue operations, and load lifting has increased interests in efficient aerial transportation solutions [1]. Being able to apply aerial robots to logistics and transportation would not only reduce costs and enhance efficiency, but also allow to reduce the burden on ground infrastructures. The application of UAVs to these fields is challenging, mainly due to their payload and battery life limitations. We address the problem of using multiple drones for payload lifting and transportation. A lot of work has been carried out on design, control and path planning for single drone transportation systems, some examples of which are [2], [3], [4], [5], [6], [7]. However, practical limitations on dimensions, vehicle complexity, load capacity, and costs limit the application of such technologies.

The widespread use and cost-effectiveness of smaller vehicles, like quadcopters, have made them the preferred choice for practical applications [8]. However, using multiple smaller vehicles in a cooperative manner, along with potential payload interactions (e.g. aerodynamic interactions, vibrations), also introduce greater complexity in terms of control and trajectory planning for cooperative aerial transportation systems [9], [10]. Connecting the vehicles to the payload through tethers is a popular choice, and allows to keep distance between drones and payload. The dynamics and control of tethered systems have been extensively investigated and yielded interesting results, e.g. [11]. Other examples are [12], which employed an interconnected structure to enhance the stability of the tethered system, or

The authors are with the Dept. of Mechanical Engineering, University of California, Berkeley {c.bosio, jerrytang, wtyng, mwm}@berkeley.edu



Fig. 1: Picture of four drones cooperatively carrying a single panel payload.

[13], which implemented a decentralized control scheme not relying on assumptions about the payload’s state. [14] presented a cooperative control approach which showed significant disturbance rejection performances. Compared to the challenges of managing tethered or moving payloads, which can be complex due to their internal dynamics and limited maneuverability, rigid attachments are often the preferred option for transportation purposes. Some work has been carried out also along this direction. [15] studied the control for cooperative payload stabilization with a team of drones equipped with grippers. [16] focused on cooperative grasped transportation control using onboard visual and inertial sensing, while [17] implemented an adaptive control framework based on a Kalman Filter for systems with uncertainty about drone location and payload parameters. [18] explores the possibility of transporting flexible payloads, taking into account internal deformations and dynamics and aiming to minimize deformations.

Our research addresses the synthesis of rigidly attached transportation systems. The core concept is to address both the design layout and the optimal control of the combined drone-payload system as one unified problem. We do this by formulating and solving an optimization problem derived from robust control theory for a first order model of the system. In particular, \mathcal{H}_2 control proved to be a promising approach to maximize disturbance rejection performances [19]. The main contribution of this research is an automated design tool to determine the optimal thrust module arrangement for payload stability and robustness. Experimentally validated with four drones, our method confirms the effectiveness of the optimal layout in rejecting disturbances.

The paper is structured as follows. In Section II we describe the mathematical framework employed to compute the optimal placement locations and the linear feedback law to control the system. We then describe the control infrastructure adopted in our hardware setup. In Section III

we show some example outputs of our optimization routine applied to different payload shapes, masses and number of drones used for transportation. In Section IV we introduce the experimental setup and the flight tests which were carried out to validate the theoretical predictions. Finally, in Section V we discuss the results, relevance of the work and future developments.

II. MATERIALS AND METHODS

The problem we solve is twofold. We i) optimize the placement of the drones on the object to be transported, so as to maximize the system's disturbance rejection performance. This involves solving an optimization problem where the cost function is derived from \mathcal{H}_2 control theory, and the decision variables are the drones' attachment locations. We then ii) address the constrained drones dynamics through a hierarchical control strategy of the integrated drone-payload system. The motion of the system is controlled using the gain obtained from the same \mathcal{H}_2 control used for layout optimization. Each drone (thrust module) is sent thrust commands. An example picture of a team of drones carrying a payload with rigid attachments is shown in Fig. 1.

A. Layout Optimization

We consider the transportation of a planar object, i.e. with a geometry which can be seen as the extrusion of a planar shape along the direction orthogonal to the plane. This assumption simplifies the mathematical derivation but does not limit significantly the space of possibilities: many objects, as delivery packages, boxes, and pallets are all included in this category. This assumption, since the drones can all lie on the same plane, is useful because it eventually simplifies both the control of the system and the layout optimization problem. In fact, each drone attachment location is described by one variable, i.e. its position along the perimeter of the payload shape. We also assume that the inertial properties of the payload are known. With reference to Fig. 2, the placement variables, are defined as $\theta = [\theta_1, \dots, \theta_N]^T$. The reference frame is defined at the geometric center of the in-plane object geometry. The drone-payload system is itself a rigid body, and can therefore be described by a state vector $\mathbf{x} = [\mathbf{p}^T, \dot{\mathbf{p}}^T, \gamma^T, \omega^T]^T \in \mathbb{R}^{12}$, where \mathbf{p} and $\dot{\mathbf{p}}$ are the position and velocity of the center of the object with respect to a global world reference frame, γ is the Roll-Pitch-Yaw triplet defining the orientation of the local frame, and ω the angular velocity with respect to the local body frame. Furthermore, each drone is seen as a thrust module providing four inputs to the system. Therefore, if N drones are deployed, we have a thrust input vector $\mathbf{u} \in \mathbb{R}^{4N}$. Due to unavoidable hardware limitations, we assume that each thrust component is limited to the interval $[u_l, u_h]$. It is possible to linearize the rigid body dynamic model about hover configuration, and decompose the inputs in $\mathbf{u} = \bar{\mathbf{u}} + \mathbf{u}'$, in which $\bar{\mathbf{u}}$ are the feedforward thrusts and \mathbf{u}' are the first order components of the linearized model. We do the same for the state vector $\mathbf{x} = \bar{\mathbf{x}} + \mathbf{x}'$. We

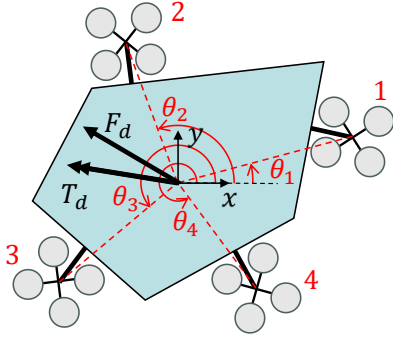


Fig. 2: Schematics of drones attached to a planar payload. Representation of the local body reference frame, placement variables θ , and disturbance actions F_d and T_d .

model the disturbances applied to the system as a random variable $\mathbf{d} = [\mathbf{F}_d^T, \mathbf{T}_d^T]^T$, in which \mathbf{F}_d and \mathbf{T}_d represent white noise force and a torque applied to the origin of the local body reference frame. The problem is formulated as the minimization of the probability of infeasible inputs when the system is subject to the defined random disturbances. We analyze the integrated drone-payload system as a whole. We can write its continuous-time linearized dynamics as:

$$\dot{\mathbf{x}}' = \mathbf{A} \mathbf{x}' + \mathbf{B}(\theta) \mathbf{u}' + \mathbf{B}_d(\theta) \mathbf{d}. \quad (1)$$

The dynamic matrix \mathbf{A} is obtained by linearization of the rigid body dynamics equations about hovering and does not depend on the placement variables θ . The matrices $\mathbf{B}(\theta)$ and $\mathbf{B}_d(\theta)$ depend on θ either directly or through the inertia of the system (which also depends on the placement variables). With reference to the \mathcal{H}_2 optimal control literature [20], we define an additional auxiliary variable:

$$\mathbf{z} = \mathbf{C} \mathbf{x} + \mathbf{D} \mathbf{u}. \quad (2)$$

The goal is to find the feedback gain K^* , such that

$$\mathbf{u} = \bar{\mathbf{u}} - K^*(\theta) \mathbf{x}' \quad (3)$$

and minimize the integral \mathcal{H}_2 control cost $J = \sum_{k=1}^6 [\int_0^\infty \mathbf{z}^T \mathbf{z} dt \text{ s.t. } d = \mathbf{e}_k \delta(t)]$, where \mathbf{e}_k is the k -th element of the euclidean base and $\delta(t)$ is Dirac's delta function. It is a known result that the optimal feedback controller is obtained as

$$K^*(\theta) = (\mathbf{D}^T \mathbf{D})^{-1} \mathbf{B}(\theta)^T \mathbf{S}_1(\theta) \quad (4)$$

where \mathbf{S} is the solution of the algebraic Riccati equation:

$$\mathbf{A}^T \mathbf{S}_1 + \mathbf{S}_1 \mathbf{A} - \mathbf{S}_1 \mathbf{B}(\mathbf{D}^T \mathbf{D})^{-1} \mathbf{B}^T \mathbf{S}_1 + \mathbf{C}^T \mathbf{C} = 0 \quad (5)$$

in which we omitted the dependency on θ for clarity of writing. The feedback gain does not depend on the matrix \mathbf{B}_d , which represents how the disturbance comes into the dynamics. The optimal cost value turns out to be:

$$J^* = \text{tr}(\mathbf{B}_d^T \mathbf{S}_1 \mathbf{B}_d). \quad (6)$$

The optimal cost value does indeed depend on the matrix \mathbf{B}_d . This is a valid cost function which can be used to optimize the drones' attachment locations. However, it does

not guarantee that the inputs generated by eq. 3 are feasible. Therefore, we make an additional step: we compute the covariance $S_2(\theta)$ of the state vector in a condition in which the optimal feedback is active and the system is subject to white noise disturbance. This can be computed using the optimal continuous-time state observer theory, which leads to the equation:

$$A_f S_2 + S_2 A_f^T + B_d B_d^T = 0 \quad (7)$$

where we defined $A_f(\theta) = A - B(\theta)K^*(\theta)$ as the dynamics matrix with linear feedback. Note that the assumption of white noise disturbance makes the process ergodic, and therefore the state sample mean is equivalent to the temporal mean. The matrix $S_2(\theta)$ is then an evaluation of the covariance of the first order state linearization \mathbf{x}' when subject to white noise disturbance. At this point we have the feed-forward thrust values, which are computed from the hovering equilibrium condition, and the covariance matrix of the inputs, obtained through the feedback law $K^*(\theta)^T S_2(\theta) K^*(\theta)$. The goal is to maximize the probability of feasible inputs. If we set the element-wise thrust lower bound to be $\mathbf{u}_l = u_l \mathbf{1}_{4N}$ and the upper bound to be $\mathbf{u}_h = u_h \mathbf{1}_{4N}$, where $\mathbf{1}_{4N}$ indicates the $4N$ -dimensional vector of ones. We can then write the optimization problem we are trying to solve as:

$$\max_{\theta} F(\mathbf{u}_h) - F(\mathbf{u}_l) \quad (8)$$

where $F(\cdot)$ is the cumulative distribution over thrust inputs, and its mean and covariance depend on θ . It is possible to compute this cost function through sampling, but the sampling approach would lead to a noisy cost function whose variance decreases linearly with the number of samples used. An additional limitation of sampling is that it needs a distribution to draw samples from, and this would have to be assumed. In addition, sampling methods are computationally expensive and lead to long solution times. Therefore, we choose to leverage the concept of minimum Mahalanobis distance [21] of the mean (feedforward thrusts) to the thrust bounds. The Mahalanobis distance of a point \mathbf{u} to a distribution with mean $\bar{\mathbf{u}}$ and covariance $\Sigma_{\mathbf{u}}$ is defined as:

$$d_M(\mathbf{u}; \bar{\mathbf{u}}, \Sigma_{\mathbf{u}}) = \sqrt{(\mathbf{u} - \bar{\mathbf{u}})^T \Sigma_{\mathbf{u}}^{-1} (\mathbf{u} - \bar{\mathbf{u}})}. \quad (9)$$

We can extend the concept of Mahalanobis distance to a hyperplane as the minimum Mahalanobis distance of a point of the hyperplane from the distribution. A two dimensional example is shown in Fig. 3. Since in our case we have a lower and an upper bound for each input, there are $8N$ different hyperplanes to check in the input space. Therefore, going back to the goal of maximizing the probability of feasible inputs, we aim to maximize the Mahalanobis distance of the mean (feedforward thrusts) to the thrust bounds. The

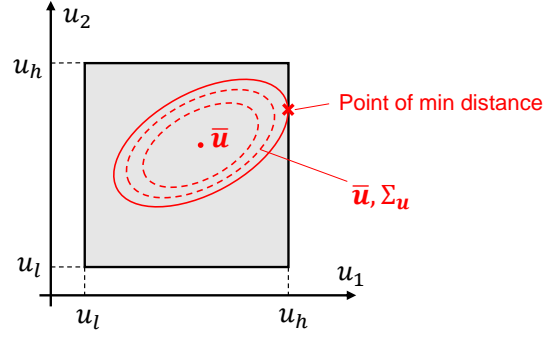


Fig. 3: Two dimensional example of minimum Mahalanobis distance to input bounds. The point of minimum distance is the point of tangency between the largest internal ellipsoid and the closest bounding hyperplane.

optimization problem can be formulated as:

$$\begin{aligned} \max_{\theta} \left\{ \min_k \left[\min_{u_a \in \{u_l, u_h\}} \left(\min_{\mathbf{u}} d_M(\mathbf{u}; \bar{\mathbf{u}}(\theta), \Sigma_{\mathbf{u}}(\theta)) \right) \right] \right\} \\ \text{s.t. } \mathbf{u}_l \leq \mathbf{u} \leq \mathbf{u}_h \text{ (element-wise)} \\ u^{(k)} = u_a \end{aligned} \quad (10)$$

In which with the superscript $u^{(k)}$ we refer to the k -th component of the vector \mathbf{u} . We are then dealing with a nested optimization problem. Trying to unpack what the routine is about: we are looking for the value θ^* which maximizes the minimum Mahalanobis distance of the thrust bounds from the feedforward thrust. This minimum distance is computed by evaluating it on each bound hyperplane separately, hence the minimization over k (component-wise) and over $u_a \in \{u_l, u_h\}$, where the subscript a stands for “active”. The inner minimization over \mathbf{u} is necessary because we are considering all the points on the active bound hyperplane, and are interested in the one with minimum distance from $\bar{\mathbf{u}}$. The optimization routine is also described in Algorithm 1. On the computational cost level, there are no particular expensive operations. Solving Riccati equations is relatively fast, and minimizing the Mahalanobis distance from a hyperplane is a Quadratic Program (QP). Therefore, for each update of θ in the optimization routine, $8N$ QPs are solved.

B. Control Infrastructure

The dynamics of motion of each drone is highly constrained due to the rigid attachments. Therefore, using a traditional drone controller would be challenging. However the integrated system corresponds itself to a rigid body (neglecting effects due to internal elasticity and vibrations). Therefore, approaching the overall dynamics and control as a whole (as was done for the placement optimization) is preferable. This strategy leads to a hierarchical control infrastructure, in which a single estimator is used for the overall motion and the drones receive thrust commands individually through N parallel communication channels. Furthermore, this control strategy comes naturally from the layout optimization computation, during which the optimal LQR gains have been computed. A block diagram of the

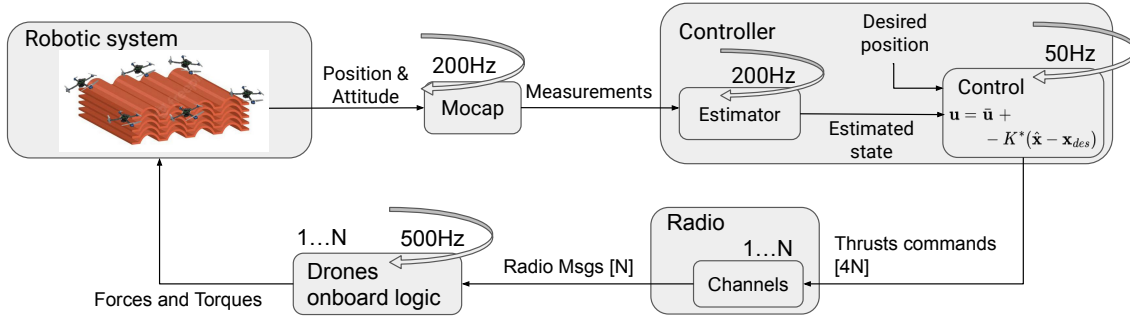


Fig. 4: Control infrastructure diagram

Algorithm 1 \mathcal{H}_2 based drone placement optimization

Require: N , drones inertia, object inertia, object shape

Require: weight matrices C and D

Initial guess for θ

while Optimization not completed **do**

 Compute overall system inertia

 Compute A , $B(\theta)$, $B_d(\theta)$ and feedforward \bar{u}

 Compute $S_1(\theta)$ and $K^*(\theta)$ from eq. 5

 Compute $S_2(\theta)$ from eq. 7

 Compute input covariance as $\Sigma_u \leftarrow K^{*T} S_2 K^*$

 Initialize d_M^*

for each thrust input component k **do**

for u_a in $\{u_l, u_h\}$ **do**

 Solve QP $d' \leftarrow \min_u d_M(u; \bar{u}, \Sigma_u)$ as in eq.

 10 s.t. $u_l \leq u \leq u_h$, $u^{(k)} = u_a$

if $d' < d_M^*$ **then**

$d_M^* \leftarrow d'$

end if

end for

end for

 Update θ

end while

suggested control infrastructure is shown in Fig. 4. The overall behavior of the controller is dominated by the choice of the matrices C and D (eq. 2), which directly impact the computation of the \mathcal{H}_2 cost. For simplicity, the C matrix was chosen to just generate a contribution to the \mathcal{H}_2 cost from the position of the system's center of mass and yaw angle (i.e. $C \in \mathbb{R}^{4 \times 12}$). After evaluating the system's behavior in simulation, we set $C(1,1) = C(2,2) = 0.5$ (corresponding to the position on a horizontal plane $x - y$), $C(3,3) = 10$ (corresponding to vertical position z), $C(4,9) = 50$ (corresponding to yaw angle), and zero for all the other components. The input contribution was set to the $2N$ -dimensional identity matrix $D = I_{2N}$.

C. Hardware Setup

The vehicles we used as a reference for layout design and eventually for experiments are quadcopters equipped with a PX-4 flight controller. The relevant vehicle parameters can be found in Tab. I. The battery capacity (5300 mAh) has been

drone size (motor to motor)	330 mm	propeller diameter	114.5 mm
drone frame mass	525 g	battery mass	437 g

TABLE I: Table of parameters

chosen to guarantee 10 minutes of flight time at maximum payload. The system theoretically is able to lift an external payload of ~ 0.8 kg per drone. It is interesting to note that the main contribution to the overall inertia of the system is due to the drones, since they are attached to the perimeter. It is interesting to note that contributing a greater inertia than the actual payload is in line with all the ground and aerial transportation systems in use nowadays.

III. RESULTS

The optimization framework which we developed allows us to determine the optimal placement of drones for transportation across many different shapes, masses and number of drones used. In Fig. 5 we show some examples of optimal placements using the vehicles described in Tab. I as a reference. It is interesting to observe that the drones are placed in a way which seems to trade off two different contributions. On the one hand, the area of the polygon defined by the drones' attachment points tends to be maximized in order to maximize control authority. On the other hand the distances of the attachment points to the system's center of mass tend to be equalized. This is an effect of employing the Mahalanobis distance as a metric. In fact, even if the control authority is maximized (i.e. the input covariance Σ_u has smaller eigenvalues), we also need the drones to have a comparable margin between feedforward thrusts \bar{u} and bounds, otherwise the Mahalanobis distance objective is decreased.

IV. EXPERIMENTAL VALIDATION

For the flight experiments the drones were attached to two different square panels of different masses and sizes. A heavier panel (A) of side length 0.61 m and mass 2.54 kg was used to test the payload capacity, and a lighter one (B) of side length 0.45 m and mass 1.088 kg to test the disturbance rejection performances. The rigid attachments have been obtained by screwing directly the drones to the

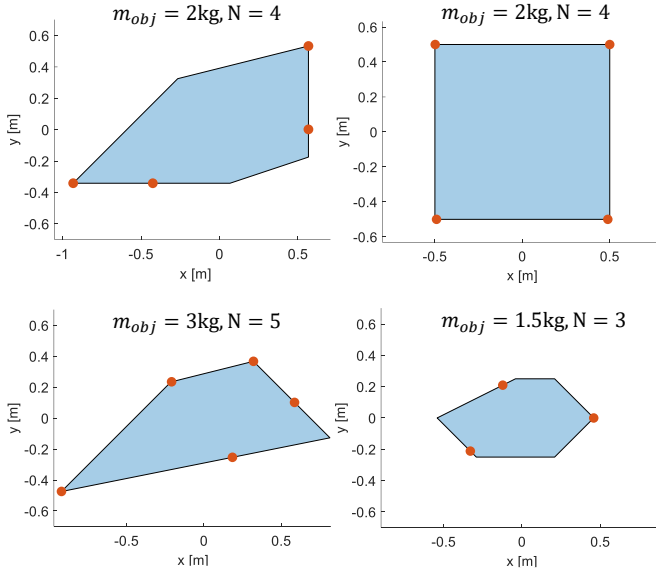


Fig. 5: Optimal layouts for various object shapes and masses using different number of drones.

panels through wood dowels. The experiments are conducted in an indoor flight space equipped with a Motion Capture system, and markers for motion tracking are placed directly on the panels.

A. Payload lifting

Panel A was used to test the payload capacity of the system. The four drones were attached to the corners of the panel and a hovering position was commanded. The system was able to successfully take off, stabilize, hover and land safely. An important observation to highlight is the close proximity of the feedforward thrusts $\bar{\mathbf{u}}$ to the upper thrust limit \mathbf{u}_h . Given the significant mass of Panel A (~ 2.5 kg) compared to the drone masses (~ 0.95 kg including battery), the narrow margin causes the system to have limited disturbance response capabilities, especially within the spatial limits of the flight space available for experiments.

B. Disturbance Rejection

The four drones were attached to panel B using two distinct configurations: an optimal one, placed at the corners, and a sub-optimal one. These configurations can be seen in Fig. 6. As a disturbance, a weight of 0.5, kg, or approximately 10% of the system's total mass, was attached to a corner of the panel during the flight, specifically under Drone 1 (Fig. 6). The mass attachment is done through a magnet to guarantee the repeatability of the experiment. Both the state and input data were collected and compared to validate their consistency with the layout optimization framework. Representative response plots over time are presented in Fig. 7.

From the data, it is clear that the choice of drone layout has a significant impact on disturbance rejection performance. The optimal layout results in lower oscillations in the attitude

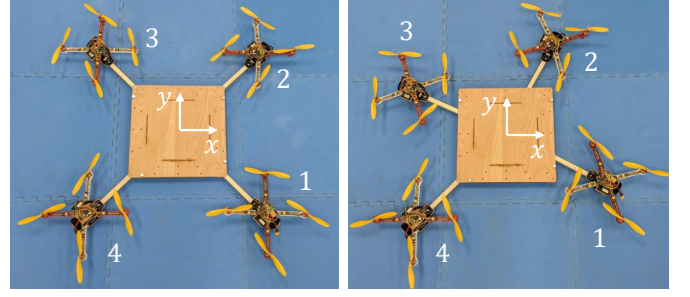


Fig. 6: Attachment layouts tested on panel B for disturbance rejection comparison. Left: optimal configuration, right: sub-optimal configuration.

of the vehicle, specifically in the pitch and roll angles, and also recovers more quickly from disturbances. In comparison, the sub-optimal layout sees its peak deviation from hovering conditions nearly double the one of the optimal setup. Another observation is related to thrust behavior after adding the payload. In the sub-optimal configuration, the increase in thrust following the addition of the payload is more noticeable. Additionally, the steady-state thrust from the drone positioned closest to the added payload is also higher in the sub-optimal setup. This suggests that, despite facing disturbances of the same magnitude, the thrust distribution becomes more uneven in the sub-optimal case, emphasizing the benefits of an optimal drone layout. It is important to note that in the sub-optimal configuration, the model and controller gains were recomputed from scratch to maximize performances (i.e. we did not use the same controller as in the optimal configuration).

V. CONCLUSIONS

In this study, we introduced a novel approach to cooperative aerial transportation with a team of drones, employing optimal control theory and a hierarchical control strategy. This methodology offers an original approach in which the layout design and control problems are solved in a coupled way through an optimization routine derived from \mathcal{H}_2 control theory. Our optimization framework allows to cater our system to different payload shapes, inertias, and drone counts. The hierarchical control structure offers a systematic and simple way to deal with the dynamics viewing the system as a single, integrated rigid body. The choice of the weight matrices C and D represents the freedom given to the control designer to obtain the desired performances. Overall, the main contributions of this paper are:

- An automated tool to optimally arrange thrust modules on a payload to maximize robustness of the integrated system;
- A control framework general enough to be able to fly different payload shapes using masses the preferred number of drones.

We also emphasize the idea that dealing with system design and control in a coupled manner simplifies the control complexity and increases the overall system performances

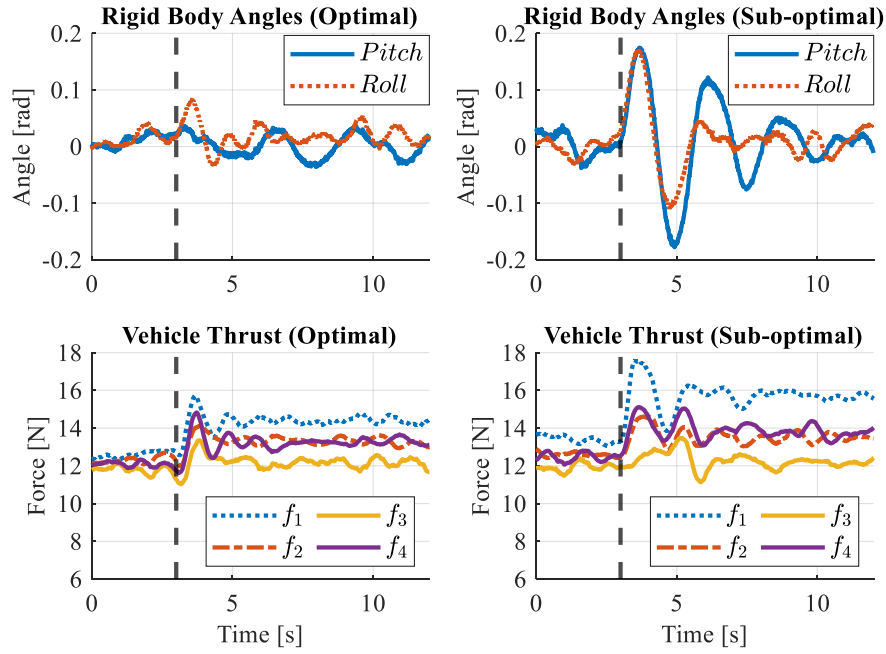


Fig. 7: Response to step disturbance over time. The mass is attached instantly (through a magnet) underneath Drone 1. The attachment time is indicated with a vertical dashed line. On the top row, attitude response. On the bottom row, total quadcopter thrusts. Left: optimal configuration, right: sub-optimal configuration

compared to a sequential siloed approach (control design following system design).

Experimental results validate the effectiveness of our approach. Flight tests under disturbance highlighted the stability and robustness of the system, and, most importantly, the agreement between the performance predicted by our optimization tool and experimental evidence.

Future developments for this work include:

- Exploring more advanced control strategies and infrastructures. At this stage, for example, the vehicles' onboard sensor data were not used.
- Removing the assumption of known payload inertia and developing a control scheme under this uncertainty component.
- Using the system as a moving tray that can be used to transport and balance a payload placed on its top.

In conclusion, this study highlights the coupling between design variables and control. The physical placement of drones significantly affect the performances of the controller. Optimizing the layout allows to take more advantage of optimal control tools rather than applying them at a second stage, once the design process is finished.

VI. ACKNOWLEDGMENTS

This work was funded by the Tsinghua-Berkeley-Shenzhen Institute (TBSI). The authors would also like to thank Roman Ibrahimov and Ruiqi Zhang for their precious help.

REFERENCES

- [1] D. K. Villa, A. S. Brandao, and M. Sarcinelli-Filho, "A survey on load transportation using multirotor uavs," *Journal of Intelligent & Robotic Systems*, vol. 98, pp. 267–296, 2020.
- [2] B. Arbanas, A. Ivanovic, M. Car, T. Haus, M. Orsag, T. Petrovic, and S. Bogdan, "Aerial-ground robotic system for autonomous delivery tasks," in *2016 IEEE international conference on robotics and automation (ICRA)*. IEEE, 2016, pp. 5463–5468.
- [3] J. Zeng, P. Kotaru, M. W. Mueller, and K. Sreenath, "Differential flatness based path planning with direct collocation on hybrid modes for a quadrotor with a cable-suspended payload," *IEEE Robotics and Automation Letters*, vol. 5, no. 2, pp. 3074–3081, 2020.
- [4] F. Schiano, P. M. Kornatowski, L. Cencetti, and D. Floreano, "Re-configurable drone system for transportation of parcels with variable mass and size," *IEEE Robotics and Automation Letters*, vol. 7, no. 4, pp. 12 150–12 157, 2022.
- [5] S. Lee and H. Lee, "Trajectory generation of a quadrotor transporting a bulky payload in the cluttered environments," *IEEE Access*, vol. 10, pp. 31 586–31 594, 2022.
- [6] M. Moshref-Javadi and M. Winkenbach, "Applications and research avenues for drone-based models in logistics: A classification and review," *Expert Systems with Applications*, vol. 177, p. 114854, 2021.
- [7] G. Macrina, L. D. P. Pugliese, F. Guerriero, and G. Laporte, "Drone-aided routing: A literature review," *Transportation Research Part C: Emerging Technologies*, vol. 120, p. 102762, 2020.
- [8] M. W. Mueller, S. J. Lee, and R. D'Andrea, "Design and control of drones," *Annual Review of Control, Robotics, and Autonomous Systems*, vol. 5, no. 1, pp. 161–177, 2022.
- [9] H. Lee, H. Kim, and H. J. Kim, "Planning and control for collision-free cooperative aerial transportation," *IEEE Transactions on Automation Science and Engineering*, vol. 15, no. 1, pp. 189–201, 2016.
- [10] H. Lee, H. Kim, W. Kim, and H. J. Kim, "An integrated framework for cooperative aerial manipulators in unknown environments," *IEEE Robotics and Automation Letters*, vol. 3, no. 3, pp. 2307–2314, 2018.
- [11] C. Meissen, K. Klausen, M. Arca, T. I. Fossen, and A. Packard, "Passivity-based formation control for uavs with a suspended load," *IFAC-PapersOnLine*, vol. 50, no. 1, pp. 13 150–13 155, 2017.
- [12] H. Rastgoftar and E. M. Atkins, "Cooperative aerial lift and manipulation (calm)," *Aerospace Science and Technology*, vol. 82, pp. 105–118, 2018.
- [13] K. Mohammadi, M. Jafarinasab, S. Sirouspour, and E. Dyer, "Decentralized motion control in a cabled-based multi-drone load transport

- system,” in *2018 IEEE/RSJ International Conference on Intelligent Robots and Systems (IROS)*. IEEE, 2018, pp. 4198–4203.
- [14] J. Geng and J. W. Langelaan, “Implementation and demonstration of coordinated transport of a slung load by a team of rotorcraft,” in *AIAA Scitech 2019 Forum*, 2019, p. 0913.
 - [15] D. Mellinger, M. Shomin, N. Michael, and V. Kumar, “Cooperative grasping and transport using multiple quadrotors,” in *Distributed Autonomous Robotic Systems: The 10th International Symposium*. Springer, 2013, pp. 545–558.
 - [16] G. Loianno and V. Kumar, “Cooperative transportation using small quadrotors using monocular vision and inertial sensing,” *IEEE Robotics and Automation Letters*, vol. 3, no. 2, pp. 680–687, 2017.
 - [17] K. Webb and J. Rogers, “Adaptive control design for multi-uav cooperative lift systems,” *Journal of Aircraft*, vol. 58, no. 6, pp. 1302–1322, 2021.
 - [18] R. Ritz and R. D’Andrea, “Carrying a flexible payload with multiple flying vehicles,” in *2013 IEEE/RSJ International Conference on Intelligent Robots and Systems*. IEEE, 2013, pp. 3465–3471.
 - [19] N. Bucki and M. W. Mueller, “A novel multicopter with improved torque disturbance rejection through added angular momentum,” *International Journal of Intelligent Robotics and Applications*, vol. 3, no. 2, pp. 131–143, 2019.
 - [20] G. E. Dullerud and F. Paganini, *A course in robust control theory: a convex approach*. Springer Science & Business Media, 2013, vol. 36.
 - [21] P. C. Mahalanobis, “On the generalized distance in statistics,” *Sankhyā: The Indian Journal of Statistics, Series A (2008-)*, vol. 80, pp. S1–S7, 2018.